Towards perfect cloaking - combining cloaks for enhanced invisibility in water waveguide systems

Author Names(s): Daria Zyla-Jablonska, Tomasz Bobinski
Division of Aerodynamics, Faculty of Power and Aeronautical Engineering,
Warsaw University of Technology, Poland
daria.zyla.dokt@pw.edu.pl

1 INTRODUCTION

Surface water waves interacting with an impermeable object scatter wave energy and generate hydrodynamic loads [1] on the structure, making the minimization of scattered energy from surface-piercing bodies a key problem in coastal and ocean [2]. The phenomenon of minimizing or eliminating the total scattered field is termed cloaking, and one effective way to achieve it is via metamaterial-inspired designs that have already enabled advanced wave-control concepts in electromagnetism, acoustics, elastodynamics, and surface water waves [3]. In this work, we consider a surface-piercing impermeable cylinder positioned on the channel centerline and focus on reducing its broadband scattering signature. Previous cloaking attempts for such cylinders have employed variable bathymetry [4] [5], floating composite plates [6], modified waveguide walls [7], or arrays of auxiliary cylinders [8]; however, most of these devices either cloak only at a single frequency or, in broadband configurations, reduce backscattered energy without recovering the phase of the transmitted wave, and typically rely on only one type of geometric modification. This work investigates broadband cloaking of a surface-piercing cylinder by jointly optimizing channel-wall shape and bathymetry and assessing whether this hybrid design outperforms single-method cloaks in minimizing the total scattered field over a wide frequency range.

2 METHODS

We consider linear surface water waves in the harmonic regime, restricted to the frequency range where only the plane mode propagates, so that the velocity potential is written as $\Phi(x, y, z, t) = \mathrm{Re}\big(\Phi(x, y, z) \cdot e^{-i\omega t}\big)$. The propagation of linear surface water waves is modelled using either (i) the non-dispersive linear shallow-water equation under the long-wave approximation ($kh \ll 1$),

$$\nabla \cdot (h \nabla \eta) + \frac{\omega^2}{g} \eta = 0 \tag{1}$$

or (ii) the mild-slope equation, under the assumption of a mild bed slope ($\|\nabla h/(kh)\| \ll 1$), which incorporates weak dispersion effects

$$\nabla \cdot (c_p c_g \nabla \eta) + k^2 c_p c_g \, \eta = 0 \tag{2}$$

where η is the free-surface elevation, k the wavenumber, h the water depth, and c_p and c_g the phase and group velocities, related through $\omega^2 = gk \tanh(kh)$. In the reference case, waves propagate in a straight waveguide of width L with a flat bottom and a surface-piercing cylinder of diameter $D = 0.6L$ centered at the origin. For the considered frequency range, the far-field solutions of (Eq.1) and (Eq.2) can be written as

$$\eta(x) = \begin{cases} Ae^{ikx} + ARe^{-ikx} & x \to -\infty \\ ATe^{ikx} & x \to +\infty \end{cases} \tag{3}$$

where A is the incident wave amplitude, and R and T denote the reflection and transmission coefficients, respectively.

The objective is to cloak the cylinder over a broad frequency range by combining variable-depth bathymetry and waveguide wall shaping. The objective function, quantifying the total scattered energy over the wavenumber range $\tilde{k} = kL/\pi \in [0.01, 1.8]$, is

$$\chi_{sc} = \frac{\int \left(|R|^2 + |T-1|^2\right) d\tilde{k}}{\int \left(|R_0|^2 + |T_0-1|^2\right) d\tilde{k}} \tag{4}$$

where the subscript 0 denotes coefficients for the reference configuration. The optimization simultaneously adjusts the channel bottom and walls to minimize the scattering coefficient χ_{sc}.

The walls are shaped according to the geometry proposed in [7] (Fig.1c), whereas the bathymetry is either (i) stepped and axisymmetric (Fig.1a), or (ii) smooth (Fig.1b), given by a function proposed in [5]

$$h(r,\theta) = h_0\left(1 + 2a_0\left(\frac{b-r}{b-D/2}\right)^2 + 2a_1\left(\frac{b-r}{b-D/2}\right)^2 \cos(2\theta)\right) \tag{5}$$

where h_0 is the still-water depth, a_0 and a_1 are geometric coefficients, and b sets the cloaking region size. For stepped (structural) bathymetry, the linear shallow-water equation is used as the governing equation, whereas for smooth geometries, the mild-slope equation is employed. The cloaking device optimization process involves an iterative design of the system configuration (bathymetry and wall geometry), solving the governing equation, and evaluating the objective function. We employ a surrogate optimization algorithm implemented in MATLAB to minimize χ_{sc}.

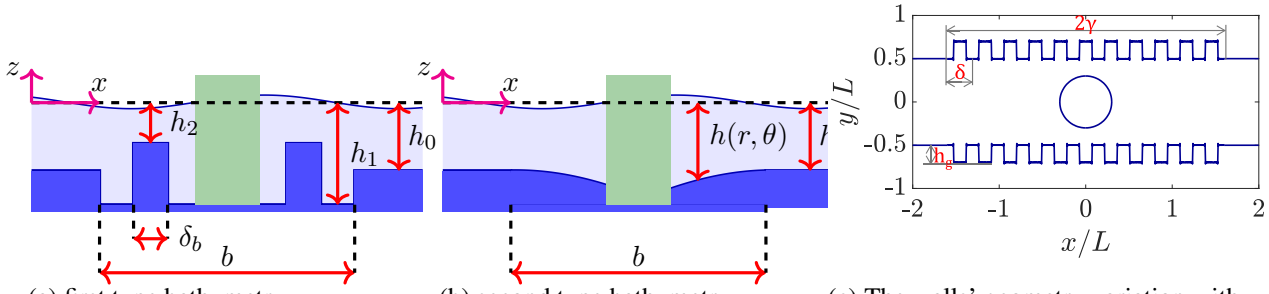

(a) first type bathymetry (stepped, axisymmetric) with unknowns h_1, h_2, δ_b, b

(b) second type bathymetry (smooth, cosine) with unknowns b, a_0, a_1

(c) The walls' geometry variation with unknowns h_g, δ, γ and n (number of terms in the cosine series) [7]

Figure 1: Investigated system configurations

RESULTS

Following the methodology described above, the objective function $X_{sc}(\mathbf{X})$ was minimized with respect to the geometry vector $\mathbf{X}$, which parametrizes the bottom and wall shapes. For smooth bathymetry, $\mathbf{X} = (b, a_0, a_1, h_g, \delta, \gamma, n)$, whereas for structured bathymetry, $\mathbf{X} = (b, h_1, h_2, \delta_b, h_g, \delta, \gamma, n)$. The optimal objective-function values are $\chi_{sc} = 0.0348$ (smooth bathymetry) and $\chi_{sc} = 0.0221$ (structured bathymetry), corresponding to a reduction of the total scattered energy by at least a factor of 25 relative to the reference configuration over the wavenumber interval $kL/\pi \leq 1.8$. These broadband reductions confirm the effectiveness of the optimized cloaking devices over the entire investigated frequency band. The associated optimal geometries are

(i) $\mathbf{X} = (0.5895, 0.7512, -0.5688, 0.1459, 1.5599, 0.8371, 19)$ for the smooth bathymetry and

(ii) $\mathbf{X} = (0.4316, 2.2635, 0.0872, 0.8450, 0.1681, 1.4317, 0.7324, 3)$ for structured bathymetry,

as shown in (Fig.2a) and (Fig.2b). Figures (Fig.2a-2c) display the reflection coefficient R, the transmission coefficient T, and the deviation of the complex transmission coefficient from that of an unperturbed wave $|T-1|$, respectively, demonstrating that $|R| < 0.16$ for $\tilde{k} \leq 1.8$ (reflected energy below 3%) while $|T| \approx 1$ and the downstream wave parameters are maintained close to the incident wave values.

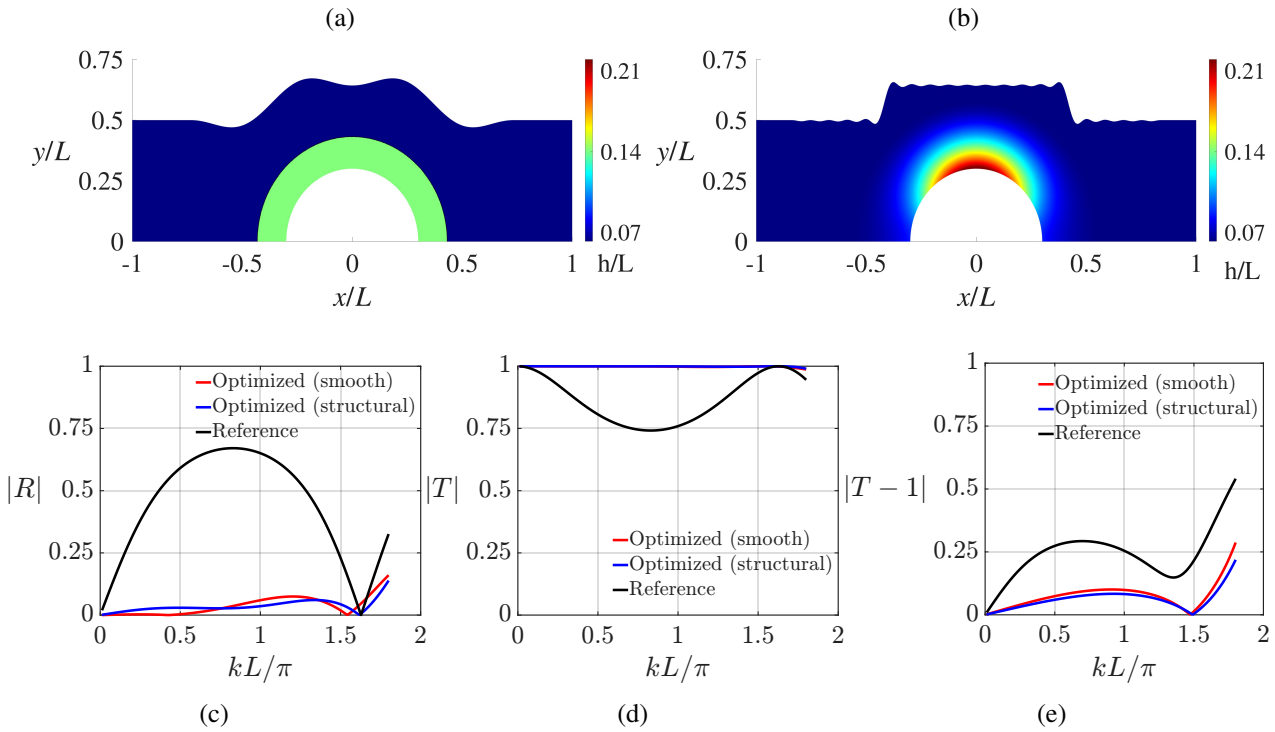

Figure 2: Figures a) and b) show optimized geometries; c), d), and e) show reflection $|R|$, transmission coefficient $|T|$ and $|T-1|$ factor, respectively.

EXPERIMENTAL VALIDATION

To verify numerical predictions, experiments were conducted in the setup shown in (Fig.3). The facility consists of a straight channel with vertical walls, a digitally controlled LinMot wavemaker, a cylindrical obstacle, cloaking devices in both variants, an absorbing beach, a light source, and two BASLER cameras. The still-water depth is $h = 1\text{cm} \pm 0.05\text{cm}$, the waveguide width is $L = 16$ cm, and the obstacle diameter is $D = 9.6\text{cm}$. Using the LinMot actuator, we generate waves in the frequency range $f \in [0.578; 1.73]$ Hz, corresponding to $\tilde{k} \in [0.6; 1.8]$, which overlap the broadband regime used in the numerical optimization. Free-surface deformations are reconstructed by combining two techniques: the optical flow (OF) method [9], used to determine the displacements relative to a reference image, and the Synthetic Schlieren (SS) method, following the approach of Moisy [10], which converts these displacement fields into the free-surface elevation profile.

DISCUSSION AND CONCLUSIONS

This study presents a novel cloaking device design achieved by simultaneously integrating two existing cloaking methods. This combined strategy effectively cloaks a cylinder positioned along the centerline of the channel in a straight, flat-bottomed waveguide by minimizing the total scattered field. This approach outperforms previous studies [7] through the combined use of two established cloaking techniques and the explicit control of the phase shift behind the cylinder. Compared with the reference configuration, the optimized device reduces the total scattered energy by a factor exceeding 25 over the targeted broadband range, and by almost a factor of 7 relative to previous cloaking designs [7], while operating over nearly twice their frequency range, making the present device significantly more broadband. Taken together, these results show that combining different cloaking techniques is an effective strategy that substantially broadens design possibilities.

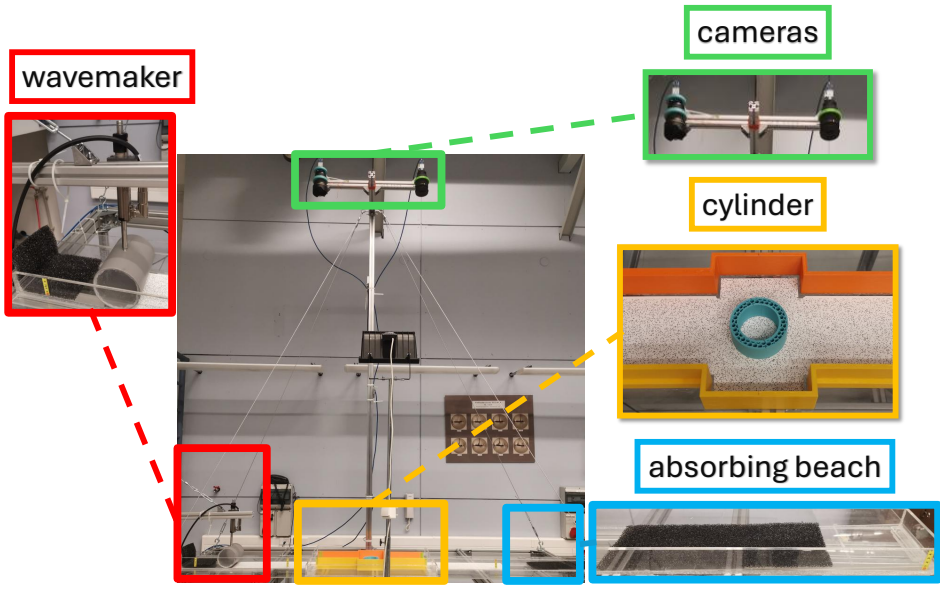

Figure 3: Experimental setup

Funding This research was funded in whole by the National Science Centre Poland, under agreement UMO-2020/39/D/ST8/01.

REFERENCES

[1] Peregrine, D.H., (2003). *Water-wave impact on walls.* Annual review of fluid mechanics, 35(1), pp.23-43.

[2] Journee, J.M. and Massie, W.W., (2000). *Offshore hydromechanics.*

[3] Zhu, S., Zhao, X., Han, L., Zi, J., Hu, X. and Chen, H., (2024). *Controlling water waves with artificial structures.* Nature Reviews Physics, 6(4), pp.231-245.

[4] Porter, R. Newman, J. N. (2014) *Cloaking of a vertical cylinder in waves using variable bathymetry.*Journal of Fluid Mechanics 750, 124−143.

[5] Bobinski, T., Maurel, A., Petitjeans, P. and Pagneux, V., (2018). *Backscattering reduction for resonating obstacle in water-wave channel.* Journal of Fluid Mechanics, 845, R4.

[6] Iida, Takahito, Zareei, Ahma, Alam, Mohammad-Reza (2023) *Water wave cloaking using a floating composite plate.* Journal of Fluid Mechanics 954, A4.

[7] Zyla, D. and Bobinski, T., (2025). *Cloaking waveguide defects at low frequencies using local wall deformations.* Journal of Fluid Mechanics, 1006, p.A26.

[8] Newman, J.N. (2014) *Cloaking a circular cylinder in water waves.* European Journal of Mechanics -B/Fluids 47, 145−150.

[9] Farneback, G. (2003). *Two-Frame Motion Estimation Based on Polynomial Expansion.* Bigun, J., Gustavsson, T. (eds) Image Analysis. SCIA 2003. Lecture Notes in Computer Science, vol 2749.

[10] Moisy, F., Rabaud, M., Salsac, K. (2009). *A synthetic Schlieren method for the measurement of the topography of a liquid interface.* Experiments in Fluids 46. 1021-1036.